Bioresource Technology 435 (2025) 132858

Contents lists available at ScienceDirect

Bioresource Technology

journal homepage: www.elsevier.com/locate/biortech

Reprogramming yeast metabolism to Alter fatty acid profiles from even-chain to odd-chain Configuration

Qiongyu Meng [a,1], Wentao Ding [a,b,1], Haiyang Cui [c], Junyang Wang [a,d], Huimin Zhao [c,*], Shuobo Shi [a,e,**]

[a] Beijing Advanced Innovation Center for Soft Matter Science and Engineering, College of Life Science and Technology, Beijing University of Chemical Technology, Beijing, PR China
[b] Key Laboratory of Food Nutrition and Safety, Ministry of Education, College of Food Engineering and Biotechnology, Tianjin University of Science and Technology, Tianjin, PR China
[c] Department of Chemical and Biomolecular Engineering, Carl R. Woese Institute for Genomic Biology, University of Illinois at Urbana-Champaign, Urbana, USA
[d] State Key Laboratory of Microbial Resources, Institute of Microbiology, Chinese Academy of Sciences, Beijing 100101, PR China
[e] State Key Laboratory of Green Biomanufacturing, Beijing University of Chemical Technology, Beijing, China

HIGHLIGHTS

- Reaching a *de novo* synthesis ratio of odd-chain FAs up to 51.9% in *S. cerevisiae*.
- Reaching highest titres in producing triglycerides and free FA in odd-chain style.
- Structure simulations revealed different FAS binding affinities for propionyl-CoA.
- Establishing the first *S. cerevisiae* with an odd-chain-dominant lipid landscape.

GRAPHICAL ABSTRACT

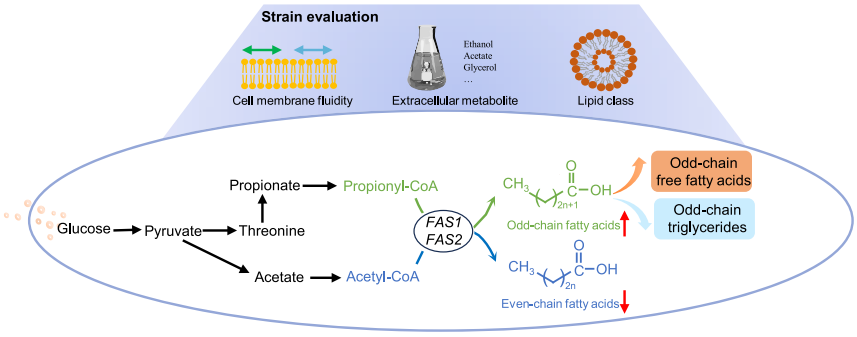

ARTICLE INFO

Keywords:
Odd-chain fatty acid derivatives
Synthetic biology
Propionyl-CoA
Fatty acid synthase
Threonine

ABSTRACT

Odd-chain fatty acids have significant applications in biofuels and pharmaceutical industries. In this study, a yeast cell factory was engineered to produce odd-chain fatty acids and their derivatives. The threonine biosynthesis pathway was initially engineered to enable the *de novo* synthesis of odd-chain fatty acids, resulting in odd-chain fatty acids accounting for 24.7 % of the total fatty acids. Subsequently, silencing the native fatty acid synthase and introducing a fatty acid synthase from *Rhodotorula toruloides*, which exhibits higher affinity for propionyl-CoA than the native enzyme, increased the proportion of odd-chain fatty acids to 51.9 %. Further modifications to the lipid metabolism enabled the production of odd-chain free fatty acids (184.1 mg/L) and odd-chain triglycerides (75.2 mg/g). This study successfully shifted the metabolism of *Saccharomyces cerevisiae*

* Corresponding author at: Department of Chemical and Biomolecular Engineering, Carl R. Woese Institute for Genomic Biology, University of Illinois at Urbana-Champaign, Urbana, USA.
** Corresponding author at: Beijing Advanced Innovation Center for Soft Matter Science and Engineering, College of Life Science and Technology, Beijing University of Chemical Technology, Beijing, PR China.
E-mail addresses: zhao5@illinois.edu (H. Zhao), shishuobo@mail.buct.edu.cn (S. Shi).
[1] These authors contributed equally to this work.

https://doi.org/10.1016/j.biortech.2025.132858
Received 16 April 2025; Received in revised form 19 June 2025; Accepted 19 June 2025
Available online 20 June 2025

from traditional even-chain fatty acids to a strain dominant in odd-chain fatty acids, demonstrating the potential to develop a novel platform strain for producing specific odd-chain fatty acids derivatives.

1. Introduction

Fatty acids are essential for the structure and function of living cells, with most being even-chain and widely used in various applications (Biermann et al., 2021). However, odd-chain fatty acids (OCFAs) are found in several species, such as ruminants, gut microorganisms, and some plants (Jenkins et al., 2017; Pfeuffer and Jaudszus, 2016). Compared with even-chain fatty acids (ECFAs), OCFAs show unique applications in the synthesis of chemicals, cosmetics, plasticizers, coatings, and biofuels, as well as the health industries (Zhang et al., 2020). Triheptanoin, the triglycerides (TAGs) form of heptanoate (C7:0), has received approval for the treatment of long-chain fatty acid oxidation disorders (Shirley, 2020). Additionally, the incorporation of OCFAs into biofuels offers the potential to enhance fuel quality and render it more comparable to petroleum-based fuels, providing greater flexibility in fuel optimization (Knothe, 2009).

Despite the diverse applications of OCFAs, their availability remains a significant challenge. Generally, OCFAs can be obtained from natural extraction, chemical synthesis, and microbial production (Avis et al., 2000). However, due to their scarcity in nature, extracting OCFAs poses a significant challenge, resulting in a waste of resources and high costs (Kim et al., 2005). Chemical synthesis of OCFAs has been rarely reported to date for commercial production. In contrast, there has been a recent demonstration of microbial production of OCFAs (Park et al., 2021). The synthesis of ECFAs starts with acetyl-CoA, while that of OCFAs start from propionyl-CoA. In nature, several pathways facilitate the synthesis of propionyl-CoA (Zhang et al., 2020). The supplementation of exogenous three-carbon compounds can serve as a substrate for the production of propionyl-CoA, which in turn enables the subsequent synthesis of OCFAs. For example, the incorporation of propionate into the medium shows significant potential for OCFAs production in *Yarrowia lipolytica*, with the highest reported titer reaching 1.9 g/L (Park et al., 2021). Meanwhile, the addition of 1-propanol has also been reported to facilitate the formation of OCFAs (Chu et al., 2020; Xu et al., 2019). However, the strategy of exogenous supplementation has been found to inhibit cell growth and increase the cost of OCFAs production. Recently, researchers have focused on exploring the *de novo* synthesis of OCFAs. Notable achievements include the production of OCFAs at a ratio of 5.6 % in *Y. lipolytica* (Park et al., 2019) and 20.3 % in *Saccharomyces cerevisiae* (Qi et al., 2023). Nonetheless, further improvements are needed to enhance both production proportion and titer to enable economically feasible industrial scale-up in the future.

S. cerevisiae holds a prominent position as an industrial microorganism for synthetic biology and biomanufacturing applications. More importantly, it exhibits exceptional capabilities in producing various fatty acid derivatives (Zhu et al., 2020). The metabolism of *S. cerevisiae* has been shifted from alcoholic fermentation to lipogenesis (Yu et al., 2018), further enhancing its significance in these fields. In this study, *S. cerevisiae* was successfully engineered to efficiently produce OCFAs and their derived products. This engineering effort shifts the predominant fatty acid composition in yeast from ECFAs to OCFAs. Specifically, the native threonine biosynthetic pathway was engineered for *de novo* propionyl-CoA synthesis, achieving a 24.7 % ratio of OCFAs production. Additionally, the affinity of various fatty acid synthases (FASs) for propionyl-CoA was evaluated, and introducing *Rhodotorula toruloides* FAS further increased the proportion of *de novo* OCFAs synthesis to 51.9 %, representing the highest ratio reported to date. The resultant OCFAs-dominant strain was shown to produce various OCFA derivatives, such as odd-chain free fatty acids (OCFFAs) and odd-chain triglycerides (OCTAGs). Despite millions of years of evolution, yeast metabolism showed high adaptability in fatty acid production: extensive engineering successfully shifted the metabolism of *S. cerevisiae* from conventional ECFAs to OCFAs, paving the way for dedicated OCFA cell factories.

2. Methods

2.1. Strains and plasmids

All strains used in this study were derived from the parental strain *S. cerevisiae* W303 (W303-1B). The plasmids and strains are listed in supplementary materials. Gene fragments and vectors were amplified and constructed in *Escherichia coli* DH5α. Gene fragments were obtained through PCR amplification of genomic DNA from the corresponding species, using Q5 High-Fidelity DNA Polymerase (New England Biolabs, NEB, Ipswich, MA, USA). The templates, primers and acquisition methods used for PCR fragments are shown in supplementary materials. The chemical transformation method of *S. cerevisiae* is also described in the literature (Qi et al., 2023).

2.2. Culture media and conditions

Yeast strains with plasmids carrying auxotrophic markers (URA, TRP, HIS) were grown in SC medium (4 % glucose) lacking the respective amino acids. Seed cultures were started in 4 mL SC medium and incubated at 30 °C, 250 rpm for 24 h, then transferred to 10 mL YPD or 10 mL minimal medium (OD600 = 0.3) in 100 mL flasks. Details of the yeast media, such as YPD, SC, and minimal media, can be found in the previous report (Zhang et al., 2019). OD600 was measured every 12 h, and fatty acids were analyzed at 60 h.

2.3. CRISPR-mediated gene integration and knockout

The CRISPR/Cas9 technology was used for gene knockout and integration. To predict the cleavage efficiency of gRNA, a computation tool in the public domain (https://atum.bio/eCommerce/cas9/input) was used. The 20 bp targeting sequences of gRNAs were combined with the pCas vector (Ding et al., 2022) using the Golden-Gate ligation technique to construct the Cas9 plasmid expression cassette with URA markers and the donor fragments. The gene integration in this study consists of two parts: pRS415-DGA1-PAH1 and gene segment $ACC1^{ser659ala,ser1157ala}$, which were inserted into the XI-2 and XII-1 sites of the W303 genome respectively (Mikkelsen et al., 2012). The sequences of primers and gRNAs used are listed in supplementary materials.

2.4. Extraction of lipids and free fatty acids

Total lipids were extracted and quantified according to the method reported in previous literature (Ferreira et al., 2018). FFAs were extracted following a previously described method (Zhu et al., 2020). During the extraction and sample preparation, a 200 μL culture solution was mixed with 40 % tetrabutylammonium hydroxide, methyl iodide, and methyl *cis*-9-tetradecenoate (C14:1) as an internal standard. The resulting samples that contained methyl esters were resuspended in 100 μL of hexane and subsequently subjected to quantification and characterization using gas chromatography–mass spectrometry (GC–MS) for FFAs.

2.5. Thin-layer chromatography for separation of lipids and quantitative detection of lipid subclasses

A previously described method with modifications was followed to separate TAGs from other fatty acid subclasses (Ferreira et al., 2018). A

small spoon of glass beads was added to the 1 mL of freeze-dried cells along with 2 mL of solution (chloroform: methanol = 2:1) and 200 μg of methyl *cis*-9-tetradecenoate (C14:1), tritetradecanoin/myristin (C14:0), cholesteryl caprylate (C8:0) standard. After extracting total lipids according to the previously reported method (Ferreira et al., 2018), 50 μL of chloroform: methanol = 2:1 solution was added to dissolve the total ester in the centrifuge tube. The mixed standards, including C14:0 TAGs (Macklin, China), C14:1 FFAs (Sigma-Aldrich, USA), C8:0 Ergosterol (SE, Macklin, China), C14:0 diacylglycerol (DAG, Macklin, China), phosphatidylethanolamine (PE, ANPEL, China), phosphatidylinositol (PI, ANPEL, China), phosphatidylcholine (PC, ANPEL, China), and phosphatidylglycerol (PG, ANPEL, China), along with the samples, were sequentially spotted onto a thin-layer chromatography (TLC) plate and then chromatographed in a glass chromatography tank. The chromatography procedure for TAGs consisted of running the plate in a mixture of chloroform–methanol-acetic acid (90:10:1, v/v/v) until 5 cm from the bottom, followed by drying and running in a mixture of hexane–ethyl ether-acetone (60:40:5, v/v/v) until 16 cm, and then again drying and running in a mixture of hexane–ethyl ether (97:3, v/v/v) until 19 cm (Fuchs et al., 2011).

To separate polar and non-polar lipids, 300 mg of freeze-dried cells were weighed and the previously described steps were repeated to extract total lipids. The chromatography procedure for non-polar lipids was *n*-hexane/ether/acetic acid: 70/30/1 (v/v/v). The chromatography procedure for polar lipids (PLs) was chloroform/methanol/acetic acid/water = 170/30/20/5 (v/v/v/v). The fluorescent yellow bright spots that corresponded to the position of polar and non-polar lipids on the chromatographic plate were scraped off and individually loaded into 15 mL centrifuge tubes. Subsequently, GC–MS analysis was performed on the subclasses of fatty acids separated by TLC after methylation according to the previously reported method (Ferreira et al., 2018) to quantify and characterize the fatty acid group in neutral lipids (NLs), FFAs, and PLs.

2.6. Protein structure analysis of fatty acid synthases

AlphaFold 2 was used for predicting the structure of *Rt*FAS, with each of the five trained model parameters from CASP14. The MSA generation, AlphaFold predictions, and structure relax with Amber were run on local server with GPU. A full database (updated to 2021–09-17) was applied for the structure predictions. According to the previous study, 3D-struture with residue 189–595 was identified as *Rt*FAS1-AT and *Sc*FAS1-AT was obtained from PDB ID: 6QL6 (residue 154–543). After obtaining the AT structures, energy minimization was performed on both structures using software YASARA Structure version 17.8.19 (Elmar and Vriend, 2014).

Molecular docking studies of propionyl-CoA were carried out to understand the catalytically competent docking poses of substrate in the binding pocket of *Rt*FAS1-AT and *Sc*FAS1-AT. The substrate structure of propionyl-CoA was obtained from PubChem and optimized with semi-empirical quantum mechanics MOPAC. For molecular docking, a grid cubic box of 15 Å was created around the active site Ser^{308} and Ser^{274} within protein *Rt*FAS1-AT and *Sc*FAS1-AT, respectively. Molecular docking calculations were performed using Autodock 4.2 Vina plug-in within YASARA Structure Version 17.4.17 (Elmar and Vriend, 2014) with a fixed protein backbone. The protein residues were treated using the AMBER ff99. The ligand atoms were treated using GAFF (Wang et al., 2004) with AM1-BCC partial charges employing particle mesh Ewald for long-range electrostatic interactions and a direct force cutoff of 10.5 Å. In total, 100 docking runs were calculated, and the obtained docking poses were clustered by applying an RMSD cutoff of 0.5 Å within the YASARA dock_run macro file (Duan et al., 2003). The proteins were visualized and analyzed using ChimeraX version 1.4 (Pettersen et al., 2021).

2.7. Gas chromatography–mass spectrometry quantification of fatty acids and their derivatives

GC–MS was employed to analyze the qualitative and quantitative aspects of fatty acids. The instrument used for this analysis was the Shimadzu GCMS-QP2020, which was equipped with a chromatographic column of DB-5 ms (30 m × 0.3 mm I.D., 0.3 μm film thickness). The GC–MS program involved the use of helium as the carrier gas and the following conditions: inlet temperature of 280 °C, total flow rate of 50 mL/min, column flow rate of 1.8 mL/min, and shunt ratio of 9. The fatty acid analysis used the microwave method (Ferreira et al., 2018). The internal standard is C14:1.

2.8. Fluorescence polarization detection

The procedure involves culturing WEP and engineered RTFATPT3 strains for 60 h, followed by cell harvesting and washing with phosphate buffer. The cells were then resuspended to an OD600 of 0.5 and stained with 2.0 μM 1,6-diphenyl-1,3,5-hexatriene (DPH) fluorescent membrane probe. After a 1 h incubation in the dark at 30 °C, the stained cells were washed and resuspended in PBS for fluorescence polarization analysis using a FLS980 series of fluorescence spectrometers (Edinburgh). The excitation wavelength is 360 nm, and the emission wavelength is 430 nm (Wang et al., 2018) (with a slit width of 2.8/2.8 nm).

Fluorescence polarization is calculated according to the following formula:

$$P = (I_{VV} - I_{VH})/(I_{VV} + 2GI_{VH}) \quad (1)$$

$$G = I_{HV}/I_{HH} \quad (2)$$

where P is fluorescence polarization values and G is the instrument grating factor. I is the corrected fluorescence intensity, and subscripts V and H represent the directions of excitation light and emission light as vertical and horizontal, respectively. At each measurement, fluorescence is corrected for background noise by subtracting the measured light intensity of the blank sample.

3. Results

3.1. Development of a de novo biosynthetic pathway for odd-chain fatty acids

By utilizing propionyl-CoA as the primer through the native fatty acid synthetic process, it becomes possible to achieve the production of OCFAs (Zhang et al., 2020). Normally, yeast can only produce trace amounts of propionyl-CoA, and the wild-type strain typically generates less than 0.8 % of OCFAs in total FAs (Qi et al., 2023). To address this challenge, a novel biosynthetic pathway for the *de novo* production of propionyl-CoA was proposed and validated, resulting in the accumulation of OCFAs (Fig. 1a).

In light of the pivotal role that propionyl-CoA plays as a crucial precursor in the biosynthesis of OCFAs, a threonine-mediated biosynthetic pathway was designed for the production of propionyl-CoA (Fig. 1a). This pathway starts from amino-acid metabolism, which naturally occurs in abundance, and has been previously reported in the production of propionate in *S. cerevisiae* (Ding et al., 2022). Since threonine is an endogenous metabolite, the pathway was initially validated by confirming the formation of propionyl-CoA through threonine degradation (see supplementary materials). The results indicated effective conversion of endogenous threonine to propionyl-CoA by expressing the propionyl-CoA synthase gene (*prpE*) from *Salmonella typhimurium* and the threonine ammonia-lyase gene (*tdcB*) from *E. coli*. Additionally, *S. cerevisiae's* endogenous fatty acid synthase (*Sc*FAS) successfully utilized propionyl-CoA as a substrate for OCFAs synthesis.

Following confirmation of its feasibility for *de novo* OCFAs synthesis,

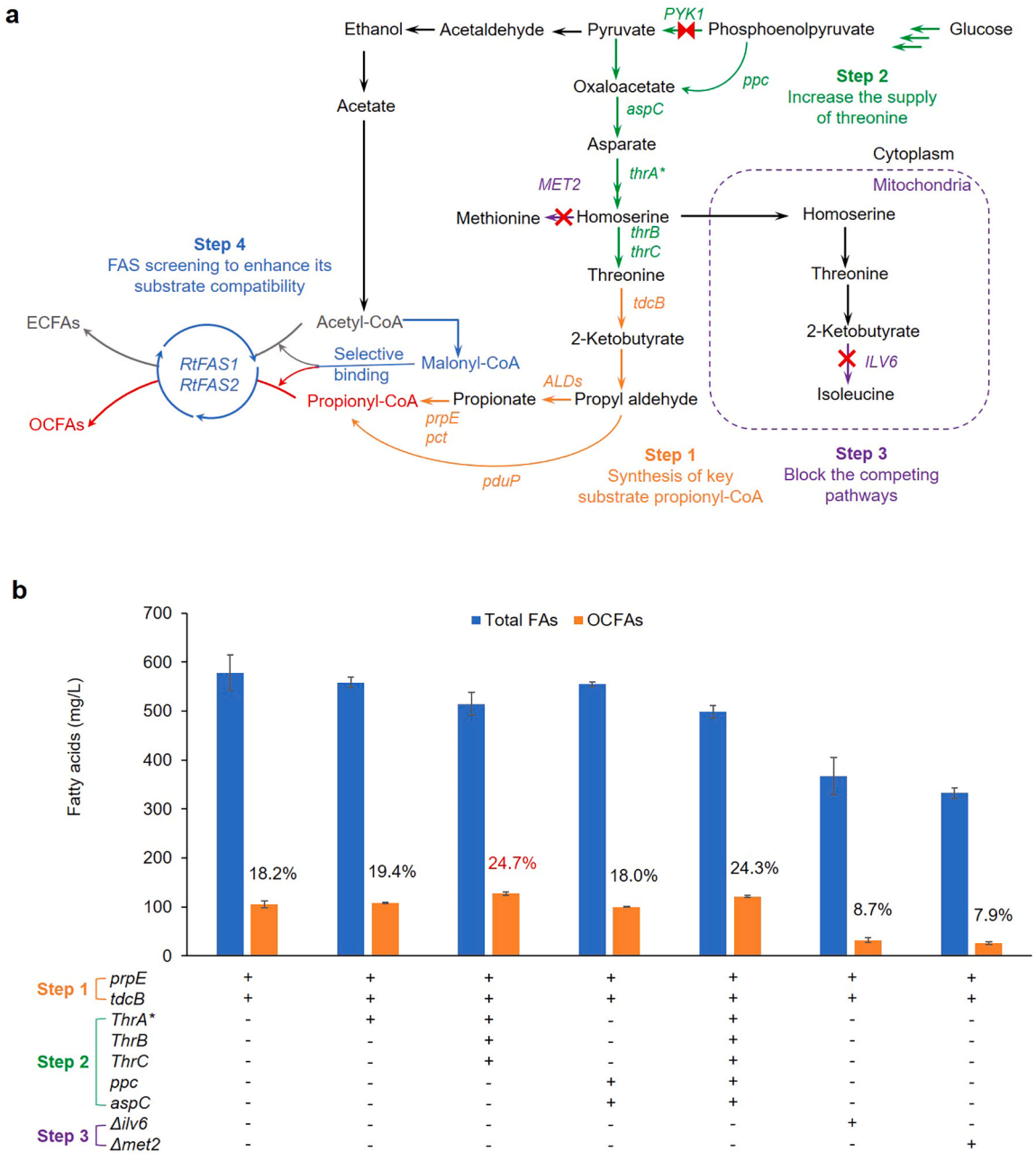

Fig. 1. Engineering the L-threonine biosynthetic pathway for improved production of odd-chain fatty acids from glucose. a Schematic overview of the metabolic pathways and metabolic engineering strategies employed within the platform strain for OCFAs production. The orange arrows represent the metabolic pathways of step 1, and the orange genes represent the target genes for metabolic engineering in step 1. The green arrows represent the metabolic pathways of step 2, and the green genes represent the target genes for metabolic engineering in step 2. The purple arrows represent the metabolic pathways of step 3, and the purple genes represent the target genes for metabolic engineering in step 3. OCFAs represent odd-chain fatty acids, and ECFAs represent even-chain fatty acids. **b** OCFAs and total FAs production from glucose by engineered *S. cerevisiae* strains with different genetic modifications. Numbers on the orange bars show the portions of OCFAs in total FAs. The red number represents the highest proportion of OCFAs produced. Data show the average of biological triplicates in YPD medium supplemented with 40 g/L glucose at 60 h (batch fermentation in 100 mL flask).

the threonine synthesis pathway in *S. cerevisiae* was systematically optimized. Initially, it was tested whether the engineered strain overexpressing *prpE* and *tdcB* could enable *de novo* production of OCFAs (see supplementary materials). In previous reports, employing a gene overexpression system for key enzymes, namely bifunctional aspartokinase I-homoserine dehydrogenase I (encoded by *thrA*), homoserine kinase (encoded by *thrB*), and threonine synthase (encoded by *thrC*), has proven effective in facilitating the conversion of aspartate into threonine (Lee et al., 2003). Noteworthy is the utilization of the mutant *thrA**, which abolishes feedback inhibition of threonine and plays a pivotal role in threonine accumulation (Ogawa Miyata et al., 2001). Drawing from these insights, multiple target genes within the threonine synthesis pathway were overexpressed in *S. cerevisiae*. This strategic intervention aims to enhance the efficiency and productivity of the glucose-to-threonine metabolic pathway, as depicted in Fig. 1a. Upon co-expression of *thrA** with *tdcB* and *prpE* genes within the threonine degradation pathway, there was a discernible elevation in the percentage of OCFAs, reaching 19.4 % (Fig. 1b). Further overexpression of *thrA** in combination with *thrB* and *thrC* not only bolstered threonine production but also yielded a noteworthy escalation in OCFAs synthesis.

The culmination of these refinements resulted in an OCFAs proportion of 24.7 % (Fig. 1b).

It has been reported that overexpression of phosphoenolpyruvate carboxylase (encoded by *ppc*) and aspartate aminotransferase (encoded by *aspC*) can increase threonine production to a certain extent (Hanke et al., 2023; Lee et al., 2007). However, the overexpression of *ppc* and *aspC* in our engineered strain did not result in an increase in either the final yield or the relative proportion of OCFAs (Fig. 1b).

To block the competing pathways and streamline carbon flux, the homoserine O-transacetylase (encoded by *MET2*) and the acetolactate synthase (encoded by *ILV6*) were knocked out. As depicted in Fig. 1b, there is no positive effect on OCFAs accumulation. To redirect carbon flux toward propionyl-CoA, pyruvate kinase gene (encoded by *PYK1*) expression was attenuated using a weaker promoter. But, this modification did not enhance OCFAs production (see supplementary materials).

Taken together, *de novo* synthesis of OCFAs was successfully achieved, with the best performance obtained through the co-expression of *tdcB*, *prpE*, *ThrA**, *ThrB* and *ThrC*. This optimization resulted in a titer of 127.5 mg/L and a composition of 24.7 %, representing a significant advancement in OCFAs production.

3.2. Selection and comparison of different fatty acid synthases for odd-chain fatty acids production

Acetyl-CoA and propionyl-CoA compete for binding to the fatty acid synthase (FAS), leading to the production of ECFAs or OCFAs, respectively (Fig. 2a). FAS typically synthesizes ECFAs, as acetyl-CoA is the preferred natural substrate (Bentley et al., 2016). It was hypothesized that the difference in FAS binding affinity for propionyl-CoA and acetyl-CoA is a crucial factor in determining the proportion of OCFAs synthesized. Therefore, selecting FAS enzymes with a higher affinity for propionyl-CoA would enhance the synthesis of OCFAs.

To identify FASs with high affinity for propionyl-CoA, several yeast species with potential for OCFAs production were selected, and cultured in media supplemented with propionate. The results indicate that three strains, namely *R. toruloides*, *Kluyveromyces lactis*, and *Lipomyces starkeyi*, produced OCFAs in a high proportion (see supplementary materials). This finding led us to hypothesize that the FASs of these three strains have a higher affinity for propionyl-CoA or that these strains themselves have a higher production level of propionyl-CoA.

Subsequently, the impact of overexpressing *FAS1/FAS2* from *R. toruloides* (*RtFAS1/RtFAS2*), *K. lactis* (*KlFAS1/KlFAS2*), and *L. starkeyi* (*LsFAS1/LsFAS2*) was investigated in a *S. cerevisiae* strain with silenced native *ScFAS1/ScFAS2,* where the original promoters were replaced with the *GAL1* promoter. As demonstrated in Fig. 2b, the expression of heterologous *RtFAS1/RtFAS2*, *KlFAS1/KlFAS2*, and *LsFAS1/LsFAS2* all successfully facilitated the production of OCFAs in *S. cerevisiae*.

The expression of *RtFAS1/RtFAS2* resulted in a significantly higher titer and ratio of OCFAs (Fig. 2b), reaching as high as 30.3 %. When *prpE*, which enhances the supply of propionyl-CoA, was co-overexpressed alongside the heterologous expression of *FAS1/FAS2*, the *RtFAS1/RtFAS2* demonstrated optimal OCFAs production at 72.2 %. This suggests that *Rt*FAS has a good affinity for propionyl-CoA and is particularly effective in enhancing *S. cerevisiae*'s ability to synthesize OCFAs.

Fas1/Fas2 are composed of several distinct domains (see supplementary materials), each with specific roles. The acyltransferase (AT) domain initiates synthesis by transferring the initial acyl group. Thus, variations in the AT functional regions of Fas1 determine the strength of their affinity with propionyl-CoA (Yu et al., 2017). Since *Rt*Fas1/*Rt*Fas2 showed the best activity in OCFAs production and the AT domain is the initial step in transferring propionyl or acetyl group to acyl carrier protein (ACP), molecular docking studies of propionyl-CoA with the AT domain of *Rt*Fas1 (*Rt*Fas1-AT) and the AT domain of *Sc*Fas1 (*Sc*Fas1-AT) were conducted to better understand the improved OCFAs production. As shown in Fig. 2c-e, although propionyl-CoA can bind closer to the active site of *Sc*Fas1-AT than to *Rt*Fas1-AT, a higher binding energy of propionyl-CoA in *Rt*Fas1-AT was observed, suggesting propionyl-CoA might have higher activity with *Rt*Fas1-AT compared to *Sc*Fas1-AT.

3.3. Improved de novo production of odd-chain fatty acids through pathway optimization

To optimize *de novo* production of OCFAs, the overexpression of heterologous *RtFAS1/RtFAS2*, encoding a FASs with high affinity for propionyl-CoA, was combined with a previously optimized threonine-mediated synthetic pathway that can supply propionyl-CoA. As shown in Fig. 3, the co-expression of *tdcB* and *prpE* genes was first combined with *RtFAS1/RtFAS2*, resulting in *de novo* synthesis of OCFAs in strain RTFATP. The concentration of OCFAs reached up to 187.6 mg/L, which accounted for 28.8 % of the total FAs produced. Subsequent overexpression of the *thrA** gene led to strain RTFATPTA*, producing 45.6 % OCFAs (294.8 mg/L). In strain RTFATPT3, the combined effects of *thrA** mutation, *thrB*, and *thrC* produced higher amounts and proportions of OCFAs (up to 51.9 %), which overturns the conventional cognition that *S. cerevisiae* mainly produces ECFAs. When using minimal medium without amino acids, the proportion of OCFAs produced by the strain RTFATPT3 remained at 51.9 %. Furthermore, the *ppc* and *aspC* genes were overexpressed in the RTFATPT3 strain, resulting in the generation of the RTFATPT5 strain. However, no enhancement in OCFAs was observed (Fig. 3a).

The dry cell weight (DCW), lipid contents and physiological parameters of key strains (WEP and RTFATPT3) were tested (Table 1). In the strain RTFATPT3, the OCFAs content increased from 0.9 mg/g to 26.8 mg/g, representing a 29.8 fold enhancement. In RTFATPT3, an unexpectedly high DCW was observed. It is hypothesized that a portion of the acetyl-CoA, which would otherwise be committed to the formation of ECFAs, was conserved and redirected towards biomass synthesis instead. The decrease in μ_{max} and the reduction in maximum specific glucose consumption rate (Table 1) may indicate a metabolic burden associated with the formation of propionyl-CoA from threonine (Van Hoek et al., 1998). A decrease in the specific production rates of acetate and ethanol in the RTFATPT3 strain typically reflects a reallocation of metabolic flux from fermentative pathways toward lipid biosynthesis (Van Hoek et al., 1998). Furthermore, the reduced specific production rate of glycerol from 0.7 mmol g^{-1} DCW h^{-1} to 0.07 mmol g^{-1} DCW h^{-1} (Table 1) may indicate a shift in cellular redox balance (Petelenz Kurdziel et al., 2013), potentially associated with increased NADPH demand during the enhanced biosynthesis of OCFAs.

To sum up, these findings suggest that metabolic engineering for OCFAs production in *S. cerevisiae* can influence central carbon metabolism and redox balance, potentially resulting in trade-offs such as reduced growth rate and fermentative output. Further investigation into these effects will be valuable for optimizing strain performance and understanding the broader implications of pathway modifications.

3.4. Evaluation of membrane fluidity in high-yield odd-chain fatty acids producing strains

PLs are a key component of all cell membranes, and alterations in FA distribution of PLs within the membrane can influence its fluidity, which is crucial for cell survival (Los et al., 2013). Therefore, the effect of OCFAs accumulation in PLs on membrane fluidity was evaluated. Table 1 shows increased fluorescence polarization in the engineered strain RTFATPT3 (0.15) compared to the control (0.10), indicating reduced membrane fluidity. This observation can be attributed to a trade-off between the increased unsaturation of fatty acids in PLs and a modest increase in average fatty acid chain length (Maertens et al., 2021). Additionally, other factors such as sterols and membrane proteins may also contribute to changes in membrane fluidity, which merit further examination.

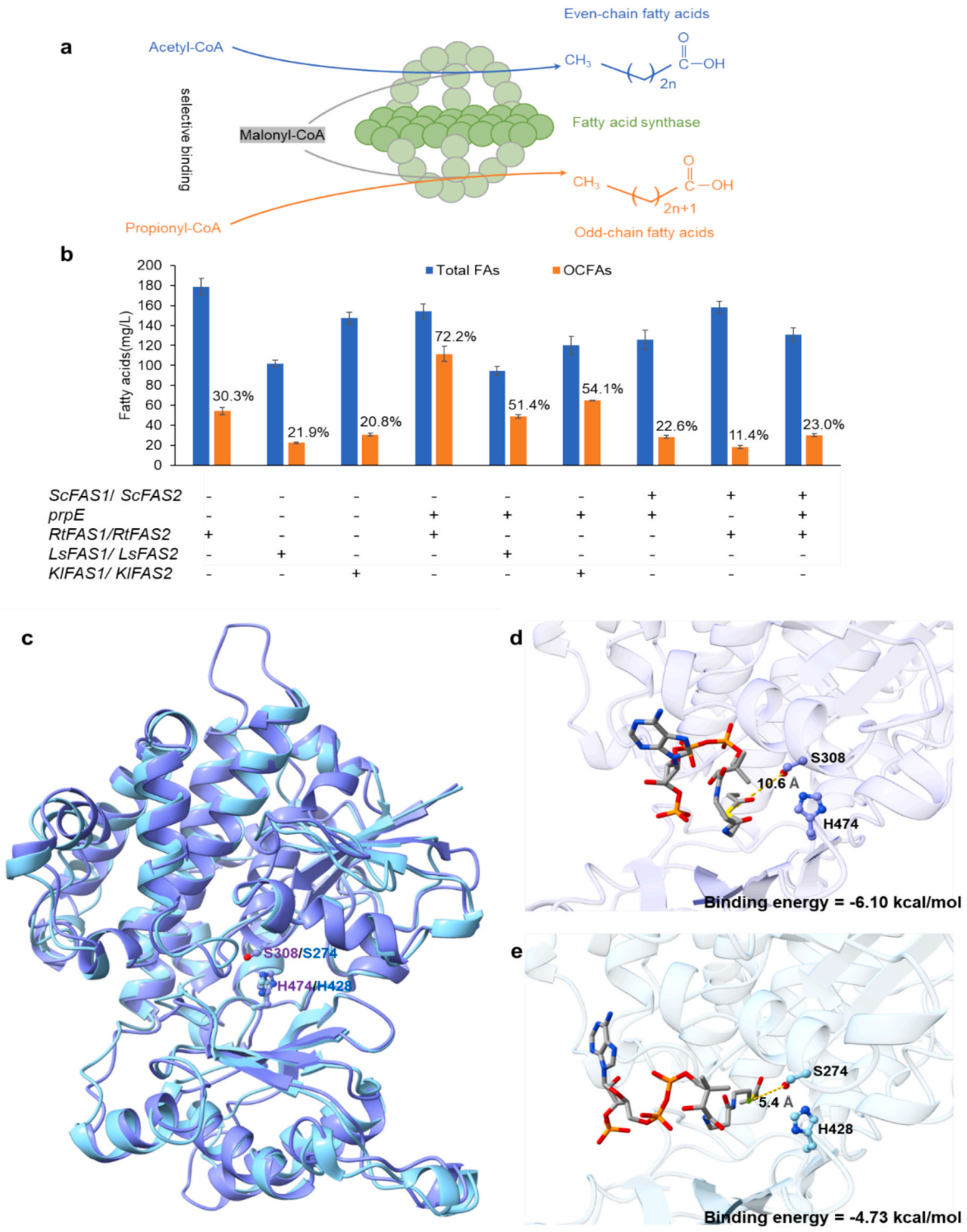

Fig. 2. Improving odd-chain fatty acids ratio through fatty acid synthase screening. a The affinity of FAS toward propionyl-CoA versus acetyl-CoA largely affects the ratio of OCFAs to ECFAs. FAS stands for fatty acid synthase, encoded by the *FAS1* and *FAS2* genes. **b** OCFAs and total FAs production from glucose and propionate by engineered *S. cerevisiae* strains overexpressing different *FAS1/FAS2* from *R. toruloides*, *K. lactis*, and *L. starkeyi*, respectively. Numbers on the orange bars show the portions of OCFAs in total FAs. Data show the average of biological triplicates in YPD medium supplemented with 40 g/L glucose and 4 g/L propionate at 60 h (batch fermentation in 100 mL flask). c Structure superimposition of *Sc*Fas1-AT and *Rt*Fas1-AT. *Sc*Fas1-AT and *Rt*Fas1-AT are shown as cartoons with colored light blue and light purple, respectively. The active site residues Ser and His in AT are shown in ball-and-stick models. The residues in *Sc*Fas1-AT are shown in blue and the corresponding ones in *Rt*Fas1-AT are shown in dark purple. A close-up view from the docking pose of propionyl-CoA in the substrate binding site of d *Rt*Fas1-AT and e *Sc*Fas1-AT from molecular docking study in a catalytically competent orientation. The *Rt*Fas1-AT (*Sc*Fas1-AT) is shown in light purple (blue) with 90 % transparency. Propionyl-CoA is shown in ball and stick representation, with carbon in dark grey, nitrogen in blue, oxygen in red, and hydrogen in grey.

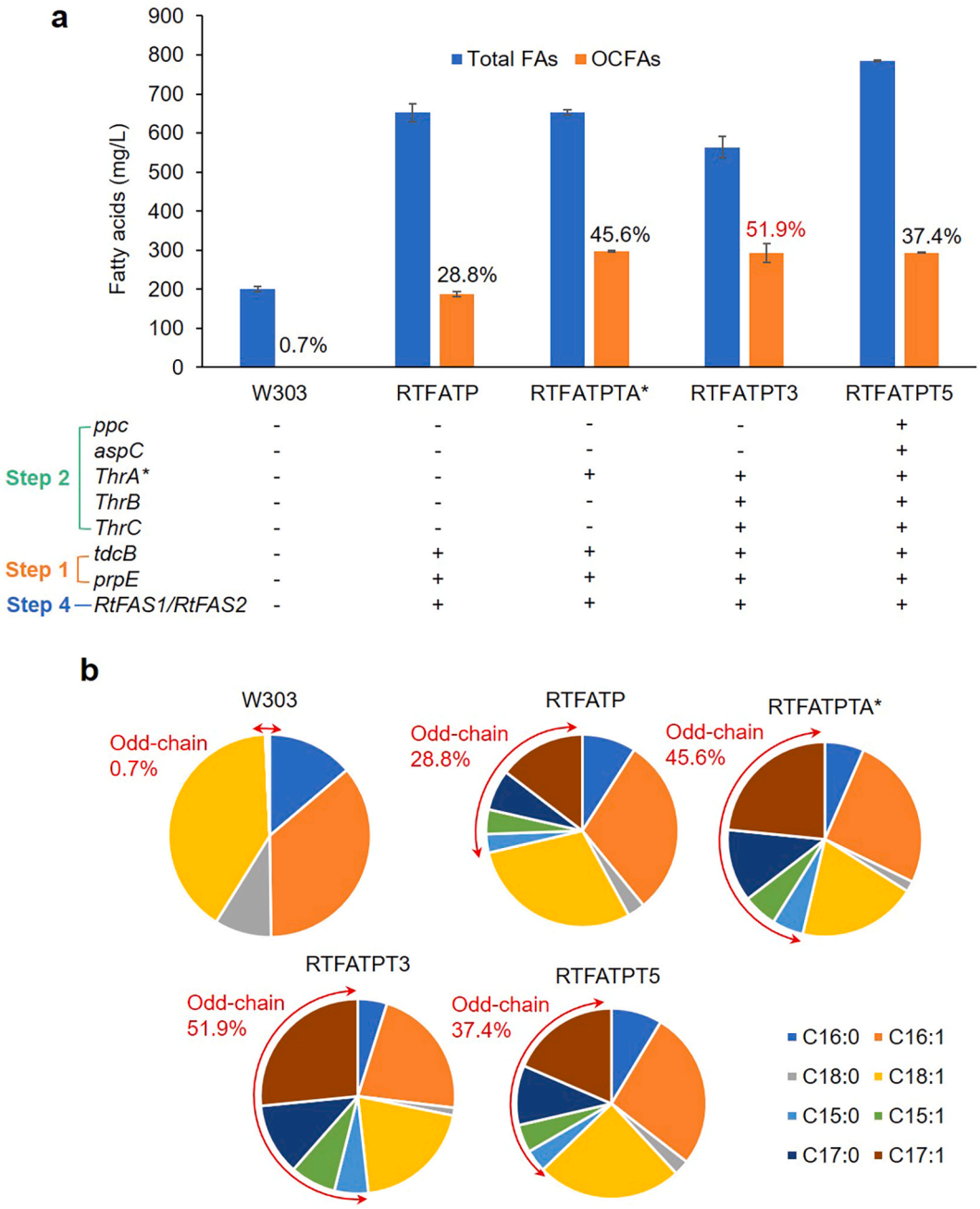

Fig. 3. Optimization of the *de novo* synthesis pathway for odd-chain fatty acids. a OCFAs and total FAs production from glucose by engineered *S. cerevisiae* strains with different genetic modifications. The proportions of OCFAs in total FAs are indicated by the numbers displayed on the orange bars. **b** The carbon chain distribution of fatty acids is determined by varying combinations of genes within the pathway responsible for synthesizing OCFAs. The data are the mean of biological triplicates obtained from 100 mL flasks containing YPD medium supplemented with 40 g/L glucose, after 60 h of batch fermentation.

The observed reduction in membrane fluidity of the engineered strain RTFATPT3 may result in decreased membrane permeability, enhancing its resistance to external disturbances. This property is critical for preserving cell integrity under specific environmental conditions (Qi et al., 2019), indicating a broader application of the OCFAs producing strain.

3.5. Distribution of subclasses of lipids in high-yielding odd-chain fatty acids strain

The significant increase in OCFAs levels in the engineered strain (RTFATPT3) suggests a potential for their incorporation into endogenous lipid metabolism. As shown in Fig. 4, NLs, PLs, and FFAs had almost undetectable or only a small amount levels of odd carbon atoms in the control strain. In contrast, all major lipid subclasses in RTFATPT3 contained detectable OCFAs, with levels reaching 46.8 % in NLs and 46.7 % in PLs. This result indicates that key enzymes involved in lipid (NLs, FFAs and PLs) metabolism, such as acyltransferases and phospholipid synthases, may accommodate OCFAs as substrates (Mora et al., 2012). This incorporation suggests that OCFAs can participate in lipid biosynthesis pathways similarly to their even-chain counterparts, though further functional validation would help clarify the extent of this substitution.

In addition, following the engineering modification for OCFAs, the predominant fatty acids in NLs in the strain RTFATPT3 (overexpression of *thrA**, *thrB*, *thrC*, *tdcB*, *prpE*, *Rt*FAS) shifted from C16:1 to C17:1 and

Table 1
Physiology evaluation of odd-chain fatty acid engineered strain RTFATPT3 and control strain WEP.

Strains	WEP[b]	RTFATPT3[b]
DCW (g/L)	5.9 ± 0.06	10.2 ± 0.8
Total fatty acids content (mg/g)	25.7 ± 6.9	51.2 ± 3.9
Odd-chain fatty acids content (mg/g)	0.9 ± 1.3	26.8 ± 1.3
Maximum specific growth rate (h^{-1})	0.55 ± 0.024	0.37 ± 0.033
Maximum specific glucose consumption rate (mmol g^{-1} DCW h^{-1})	4.7 ± 0.3	1.9 ± 0.04
Maximum specific glycerol production rate (mmol g^{-1} DCW h^{-1})	0.7 ± 0.04	0.07 ± 0.003
Maximum specific ethanol production rate (mmol g^{-1} DCW h^{-1})	12.2 ± 1.0	4.1 ± 0.7
Maximum specific acetate production rate (mmol g^{-1} DCW h^{-1})	0.1 ± 0.004	0.04 ± 0.02
Fluorescence polarization (P) values[a]	0.10 ± 0.0090	0.15 ± 0.016
Unsaturation of FA carbon chain (%)	51.3 ± 3.6	67.1 ± 1.8
Average chain length	16.2 ± 0.06	16.8 ± 0.02

[a] The excitation wavelength is 360 nm, and the emission wavelength is 430 nm (with a slit width of 2.8/2.8 nm).
[b] Data are the mean of biological triplicates obtained from 250 mL flasks containing YPD medium supplemented with 40 g/L glucose, after 60 h of batch fermentation.

the main PLs also changed from C16:0 to C17:1. The difference is markedly significant when compared to the control.

3.6. Tailoring the odd-chain fatty acids-containing strain as a platform for production of odd-chain fatty acids derivatives

Given the unique properties of OCFAs compared to ECFAs, the established OCFAs biosynthesis platform was subsequently utilized to produce various OCFAs derivatives, including odd-chain FFAs and OCTAGs. To accumulate the content of odd-chain FFAs, the *POX1* gene was knocked out to block the β-oxidation pathway. Fatty acyl-CoA synthetases, encoded by *FAA1* and *FAA4*, can activate acylation of FFAs to acyl-CoA (Ferreira et al., 2018). Therefore, genes *FAA1* and *FAA4* were knocked out to accumulate FFAs (Fig. 5a). As shown in Fig. 5c, the odd-chain FFAs of the engineering strain RTFATPT3Δ reached up to 184.1 mg/L. This is the highest titer of odd-chain FFAs *de novo* produced to date in the microbial cell factories.

Due to their metabolic degradation pathway, OCTAGs have more health benefits than even-chain TAGs (ECTAGs). For example, triheptanoin (a seven-carbon triglyceride) can be used to treat long-chain fatty acid oxidation disorders (LC-FAOD) (Mochel, 2017). Therefore, the constructed OCFAs platform strain RTFATPT3 was utilized to produce OCTAGs. To increase carbon flux towards OCTAGs synthesis, the double mutant version of $ACC1^{**}$ ($ACC1^{S659A/S1157A}$) (Yu et al., 2018) as expressed. Previous studies have indicated that lipid synthesis is largely regulated by *PAH1* is a phosphatidate phosphatase that catalyzes the dephosphorylation of phosphatidic acid (PA) to produce diacylglycerol (DAG) (Pascual and Carman, 2013). This reaction is a key branch point directing lipid intermediates toward TAG synthesis rather than membrane phospholipids. And the DAG is then acylated by acyl-CoA diacylglycerol transferase (*DGA1*) to form TAGs. Thus, *PAH1* and *DGA1* by chromosomal integration were expressed. Meanwhile, *TGL3*, *TGL4*, and *TGL5,* which are the principal TAGs lipases for catalyzing the breakdown of TAGs into fatty acids, were knocked out. Additionally, the *ARE1* gene was also knocked out, which is involved in SE synthesis. Metabolic pathway modifications are shown in Fig. 5b. The engineered strain exhibited a noteworthy elevation in the concentration of OCTAGs, reaching 75.2 mg/g. This represented a 5.3-fold increase compared with the control strain RTFATPT3 and a remarkable surge of over 100 times when compared with the control strain WEP (Fig. 5d).

4. Discussion

This work not only reports the highest *de novo* synthesis ratio of OCFAs achieved to date, thereby broadening the range of engineered OCFAs derivatives, but also laid the groundwork for the synthesis of other unconventional odd-chain compounds, such as odd-chain FFAs, medium-chain OCFAs, odd-chain dicarboxylic acids, and odd-chain waxes. The development of this OCFAs platform advances metabolic engineering, offering valuable insights into the complex biochemical pathways that regulate fatty acid biosynthesis. Moreover, it provides a fundamental basis for elucidating the interplay between fatty acid metabolism and cellular physiological processes.

OCFAs, while rare in nature and difficult to synthesize, have been linked to a wide range of applications. OCTAGs are key in energy metabolism, glucose regulation, and compound synthesis. The FDA's approval of Dojolvi (UX007/triheptanoin) in 2020 highlights the therapeutic potential of OCFAs in treating LC-FAOD (Shirley, 2020). It has been reported in the literature that *E. coli*, *Y. lipolytica*, and *Rhodococcus opacus* can synthesize OCFAs by adding propionate or propanol (Shirley, 2020; Park et al., 2021; Wu and San, 2014). However, if a large amount of propionate or propanol is added as a substrate, the production cost will be greatly increased and growth will be inhibited (Ding et al., 2022). Moreover, instances of OCFAs synthesis from glucose exist; however, the ratio of OCFAs remains modest. For example, within *Y. lipolytica*, the *de novo* synthesis of OCFAs accounts for a mere 5.6 % of the total FAs composition (Park et al., 2019). In this work, both the upstream supply pathway of propionyl-CoA and the downstream fatty acid synthase affinity for propionyl-CoA were optimized. The highest level of *de novo* synthesis of OCFAs was achieved in *S. cerevisiae*, which laid the foundation for further investigation of the efficient synthesis mechanism of OCFAs. The platform strains, which have a high proportion of OCFAs production, provide an opportunity for producing OCFA derivatives.

Previous studies have explored OCFAs production via the 3-hydroxypropionic acid (3-HP) pathway. However, the 3-HP pathway is not native to *S. cerevisiae* and requires the expression of multiple heterologous enzymes, increasing metabolic burden and potentially reducing growth and yields. Additionally, the conversion of 3-HP to propionyl-CoA is often thermodynamically or kinetically inefficient, limiting OCFAs production efficiency (Qi et al., 2023). On the other hand, FAs cleavage to produce medium-chain OCFAs suffers from significant energy loss and low conversion efficiency, leading to resource waste and minimal yields (Dong et al., 2024). Threonine, an essential amino acid widely found in various organisms, offers a more efficient route for OCFAs production. By combining threonine deaminase (*tdcB*) with the dominant gene *prpE*, carbon flux was directed toward propionyl-CoA (a precursor for OCFAs). The study also explored the threonine biosynthesis pathway, optimizing enzyme overexpression (*thrA**, *thrB*, and *thrC*) alongside *tdcB* and *prpE* to achieve a ratio of OCFAs at 24.7 %. While the key difference in producing ECFAs and OCFAs is the utilization of the initial unit for FA synthesis, various FASs were screened to identify a FAS with higher affinity for propionyl-CoA. The combination of *RtFAS1/RtFAS2* expression with modifications to the threonine synthesis pathway resulted in the highest reported proportion of *de novo* OCFAs (51.9 %) in microorganism to date, as observed in the RTFATPT3 strain. This study also presents the first exploration of FAS affinity for propionyl-CoA.

The presence of increased OCFAs suggests that the engineered yeast strains can be equipped to metabolize odd-chain substrates, forming different subclasses of lipids that contain OCFAs. Fig. 4 shows that OCFAs are primarily present in NLs, FFAs and PLs, with C17 being the most dominant odd carbon chain, followed by C15. The accumulation and utilization of odd-chain FFAs may enhance stress resistance in engineered strains by modulating cellular stress response pathways, improving survival and growth under adverse conditions (Ushio et al., 2023). According to reports, OCTAGs have more health benefits (Vockley, 2020; Mochel, 2017).

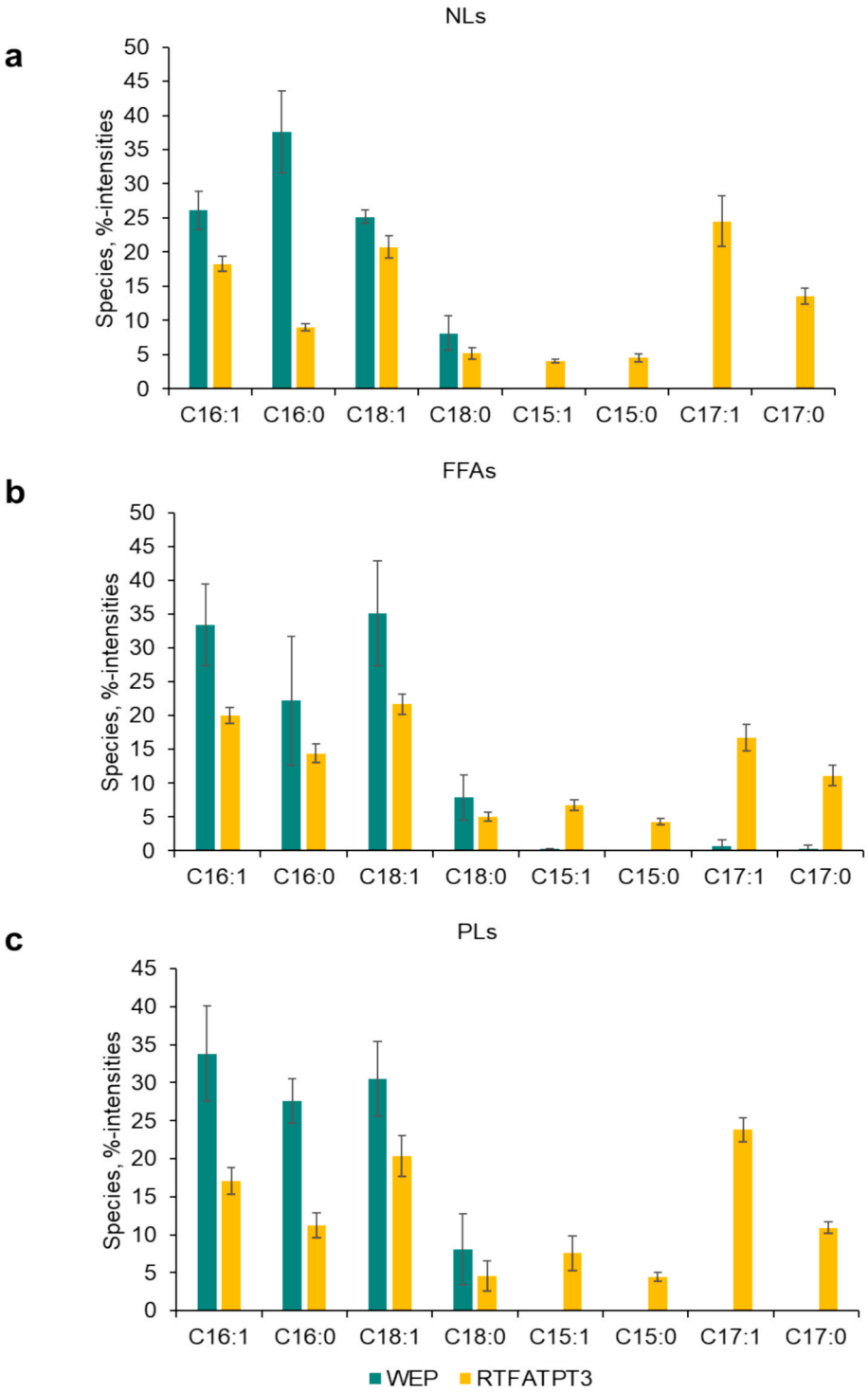

Fig. 4. Lipid subclasses profiles in odd-chain fatty acids dominant strain RTFATPT3 and the control strain WEP. a The proportion of different carbon chain fatty acids in acyl glycerides (neutral lipids, NLs); **b** The proportion of different carbon chain fatty acids in FFAs (free fatty acids); **c** The proportion of different carbon chain fatty acids in PLs (polar lipids). Data are the mean of biological quadruplicates obtained from 100 mL flasks containing YPD medium supplemented with 40 g/L glucose, after 60 h of batch fermentation.

In this work, the unique capabilities of the OCFAs platform strain RTFATPT3 were harnessed to synthesize two distinct categories of odd-chain fatty acid derivatives: OCTAGs and odd-chain FFAs. While the engineering of metabolic pathways for the production of even-chain FFAs and even-chain TAGs has been explored in prior studies (Chen et al., 2014), our endeavor represents the highest reported titer of OCFAs derivatives produced in microorganisms. While the engineered strain achieved a high intracellular OCFAs ratio, further optimization is likely required to maintain sufficient propionyl-CoA flux in high lipid-producing backgrounds. Enhancing precursor supply and improving pathway balance will be key to scaling production, as demonstrated in the previous work in converting yeast metabolism to lipogenesis (Yu et al., 2018). Additionally, the concept of extracellular fatty acid secretion presents an alternative route to alleviate intracellular lipid burden and simplify product recovery, though potential toxicity must be addressed through strain engineering. Enhancing the tolerance of yeast

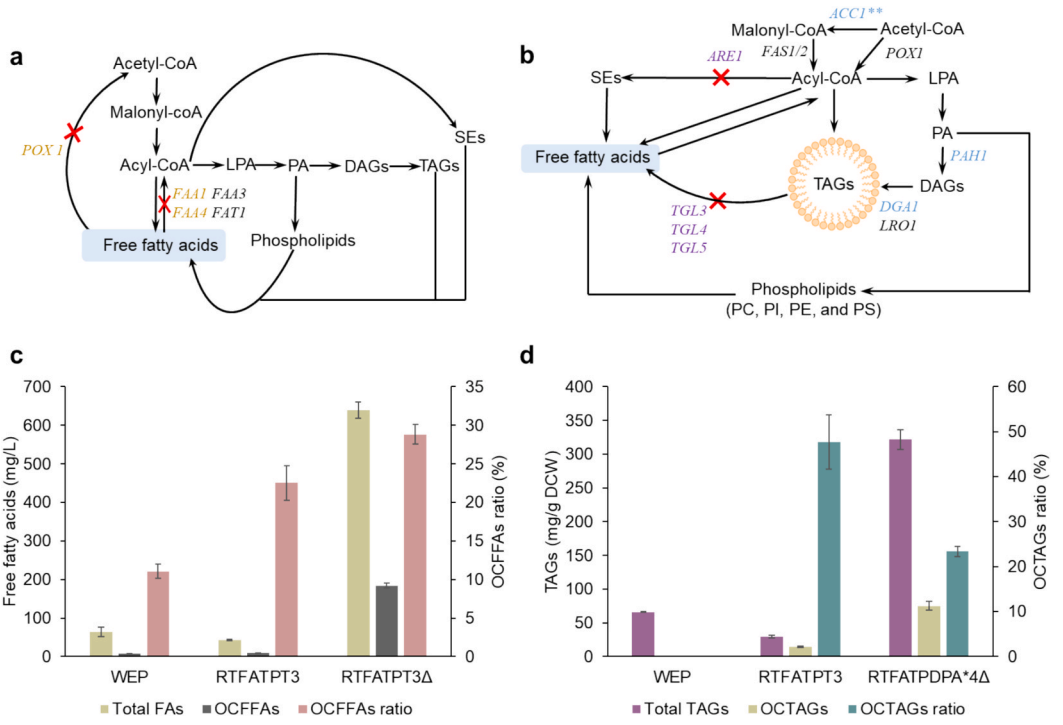

Fig. 5. Synthesis of odd-chain fatty acids derivatives using the odd-chain fatty acids platform strain. a Metabolic pathway for the synthesis of odd-chain FFAs. **b** Metabolic pathway for the synthesis of OCTAGs. **c** Level of odd-chain FFAs produced by fermentation of engineered strains. **d** Level of OCTAGs produced by fermentation of engineered strains. Data are the mean of biological triplicates obtained from 100 mL flasks containing YPD medium supplemented with 40 g/L glucose, after 60 h of batch fermentation.

to extracellular fatty acids, as well as incorporating fatty acid export systems, could be promising strategies to address these limitations (Zhu et al., 2020). Overall, our findings provide a foundation for OCFAs biosynthesis in yeast, but further efforts are needed to adapt this platform for industrial-scale OCFAs production.

5. Conclusion

This work represents a significant advancement in the *de novo* synthesis of OCFAs, achieving an unprecedented OCFA proportion of 51.9 % in *S. cerevisiae*. In addition, the production of odd-chain FFAs and OCTAGs are the highest reported to date in engineered microbial cell factories. The engineered strains serve as versatile microbial chassis, enabling efficient, scalable bioproduction of diverse OCFA derivatives. Moreover, the genetic modification of *S. cerevisiae* to enhance the production of OCFAs induced significant alterations in cellular physiology, including changes in membrane fluidity and broader metabolic shifts. These findings illuminate the complex relationship between lipid composition and cellular function.

CRediT authorship contribution statement

Qiongyu Meng: Writing – original draft, Investigation, Formal analysis, Data curation. **Wentao Ding:** Methodology, Investigation, Formal analysis. **Haiyang Cui:** Writing – original draft, Software, Methodology. **Junyang Wang:** Methodology, Investigation, Data curation. **Huimin Zhao:** Writing – review & editing, Supervision, Project administration, Funding acquisition. **Shuobo Shi:** Writing – review & editing, Supervision, Resources, Project administration, Funding acquisition.

Declaration of competing interest

The authors declare that they have no known competing financial interests or personal relationships that could have appeared to influence the work reported in this paper.

Acknowledgements

This study was financially supported by the National Natural Science Foundation of China (22278024 and 2191101491), the Fundamental Research Funds for the Central Universities, and the Beijing Advanced Innovation Center for Soft Matter Science and Engineering.

Appendix A. Supplementary data

Supplementary data to this article can be found online at https://doi.org/10.1016/j.biortech.2025.132858.

Data availability

All the gene sequences used in this work were available in NCBI by entering the species category and gene names. All other relevant raw data supporting the results of this article were listed in the Supplementary Information or available from the corresponding authors upon reasonable request.

References

Avis, T.J., Boulanger, R.R., Bélanger, R.R., 2000. Synthesis and biological characterization of (z)-9-heptadecenoic and (z)-6-methyl-9-heptadecenoic acids: fatty acids with antibiotic activity produced by *Pseudozyma flocculosa*. J. Chem. Ecol. 26, 987–1000.

Bentley, G.J., Jiang, W., Guamán, L.P., et al., 2016. Engineering *Escherichia coli* to produce branched-chain fatty acids in high percentages. Metab. Eng. 38, 148–158.

Biermann, U., Bornscheuer, U., Feussner, T.I., et al., 2021. Fatty acids and their derivatives as renewable platform molecules for the chemical industry. Angew. Chem. Int. Ed. Engl. 60, 20144–20165.

Chen, L., Zhang, J., Lee, J., et al., 2014. Enhancement of free fatty acid production in *Saccharomyces cerevisiae* by control of fatty acyl-CoA metabolism. Appl. Microbiol. Biotechnol. 98, 6739–6750.

Chu, M.Y., Zhang, L.S., Lou, W.Y., et al., 2020. Preparation and characterization of oil rich in odd chain fatty acids from *Rhodococcus opacus* PD630. J. Am. Oil Chem. Soc. 97, 25–33.
Ding, W.T., Meng, Q.Y., Dong, G.N., et al., 2022. Metabolic engineering of threonine catabolism enables *Saccharomyces cerevisiae* to produce propionate under aerobic conditions. Biotechnol. J. 17, 3.
Dong, G., Zhao, Y., Ding, W., et al., 2024. Metabolic engineering of *Saccharomyces cerevisiae* for *de novo* production of odd-numbered medium-chain fatty acids. Metab. Eng. 82, 100–109.
Duan, Y., Wu, C., Chowdhury, S., et al., 2003. A point-charge force field for molecular mechanics simulations of proteins based on condensed-phase quantum mechanical calculations. J. Comput. Chem. 24 (16), 1999–2012.
Elmar, K., Vriend, G., 2014. YASARA View—molecular graphics for all devices—from smartphones to workstations. Bioinformatics 30, 2981–2982.
Ferreira, R., Teixeira, P.G., Siewers, V., et al., 2018. Redirection of lipid flux toward phospholipids in yeast increases fatty acid turnover and secretion. P. Natl. Acad. Sci. Usa. 115, 1262–1267.
Fuchs, B., Süss, R., Teuber, K., et al., 2011. Lipid analysis by thin-layer chromatography–a review of the current state. J. Chromatogr. A 1218, 2754–2774.
Hanke, P., Parrello, B., Vasieva, O., et al., 2023. Engineering of increased L-Threonine production in bacteria by combinatorial cloning and machine learning. Metab. Eng. Commun. 17, e00225.
Jenkins, B.J., Seyssel, K., Chiu, S., et al., 2017. Odd chain fatty acids; new insights of the relationship between the gut microbiota, dietary intake, biosynthesis and glucose intolerance. Sci. Rep. 7, 44845.
Kim, E.J., Sanderson, R., Dhanoa, M.S., et al., 2005. Fatty acid profiles associated with microbial colonization of freshly ingested grass and rumen biohydrogenation. J. Dairy Sci. 88, 3220–3230.
Knothe, G., 2009. Improving biodiesel fuel properties by modifying fatty ester composition. Energ. Environ. Sci. 2, 759–766.
Lee, J.H., Lee, D.E., Lee, B.U., et al., 2003. Global analyses of transcrip-tomes and proteomes of a parent strain and an L-threonine-overproducing mutant strain. J. Bacteriol. 185, 5442–5451.
Lee, K.H., Park, J.H., Kim, T.Y., et al., 2007. Systems metabolic engineering of *Escherichia coli* for L-threonine production. Mol. Syst. Biol. 3, 149.
Los, D.A., Mironov, K.S., Allakhverdiev, S.I., et al., 2013. Regulatory role of membrane fluidity in gene expression and physiological functions. Photosynth. Res. 116, 489–509.
Maertens, J.M., Scrima, S., Lambrughi, M., et al., 2021. Molecular-dynamics-simulation-guided membrane engineering allows the increase of membrane fatty acid chain length in *Saccharomyces cerevisiae*. Sci. Rep. 11, 17333.
Mikkelsen, M.D., Buron, L.D., Salomonsen, B., et al., 2012. Microbial production of indolylglucosinolate through engineering of a multi-gene pathway in a versatile yeast expression platform. Metab. Eng. 14, 104–111.
Mochel, F., 2017. Triheptanoin for the treatment of brain energy deficit: a 14-year experience. J. Neurosci. Res. 95, 2236–2243.
Mora, G., Scharnewski, M., Fulda, M., 2012. Neutral lipid metabolism influences phospholipid synthesis and deacylation in *Saccharomyces cerevisiae*. PLoS One 7, e49269.
Ogawa Miyata, Y., Kojima, H., Sano, K.H., 2001. Mutation analysis of the feedback inhibition site of aspartokinase III of *Escherichia coli* K-12 and its use in L-threonine production. J. Agric. Chem. Soc. Jpn. 65, 1149–1154.
Park, Y.K., Bordes, F., Letisse, F., et al., 2021. Engineering precursor pools for increasing production of odd-chain fatty acids in *Yarrowia lipolytica*. Metab. Eng. Commun. 12, e00158.
Park, Y.K., Ledesma Amaro, R., Nicaud, J.M., 2019. *De novo* biosynthesis of odd-chain fatty acids in *Yarrowia lipolytica* enabled by modular pathway engineering. Front. Bioeng. Biotech. 7, 484.
Pascual, F., Carman, G.M., 2013. Phosphatidate phosphatase, a key regulator of lipid homeostasis. Biochim. Biophys. Acta 1831, 514–522.
Petelenz Kurdziel, E., Kuehn, C., Nordlander, B., et al., 2013. Quantitative analysis of glycerol accumulation, glycolysis and growth under hyper osmotic stress. PLoS Comput. Biol. 9, e1003084.
Pettersen, E.F., Goddard, T.D., Huang, C.C., et al., 2021. UCSF ChimeraX: Structure visualization for researchers, educators, and developers. Protein Sci. 30, 70–82.
Pfeuffer, M., Jaudszus, A., 2016. Pentadecanoic and heptadecanoic acids: multifaceted odd-chain fatty acids. Adv. Nutr. 7, 730–734.
Qi, N.L., Ding, W.T., Dong, G.L., et al., 2023. *De novo* bio-production of odd-chain fatty acids in *Saccharomyces cerevisiae* through a synthetic pathway via 3-hydroxypropionic acid. Biotechnol. Bioeng. 120, 852–858.
Qi, Y., Liu, H., Chen, X., et al., 2019. Engineering microbial membranes to increase stress tolerance of industrial strains. Metab. Eng. 53, 24–34.
Shirley, M., 2020. Triheptanoin: first approval. Drugs 80, 1595–1600.
Ushio, M., Ishikawa, T., Matsuura, T., et al., 2023. MHP_1 and MHL generate odd-chain fatty acids from 2-hydroxy fatty acids in sphingolipids and are related to immunity in *Arabidopsis thaliana*. Plant Sci. 336, 111840.
Van Hoek, P., Van Dijken, J.P., Pronk, J.T., 1998. Effect of specific growth rate on fermentative capacity of baker's yeast. Appl. Environ. Microbiol. 64, 4226–4233.
Vockley, J., 2020. Long-chain fatty acid oxidation disorders and current management strategies. Am. J. Manag. Care 26, 147–154.
Wang, J., Wolf, R.M., Caldwell, J.W., et al., 2004. Development and testing of a general amber force field. J. Comput. Chem. 25 (9), 1157–1174.
Wang, L.H., Zeng, X.A., Wang, M.S., et al., 2018. Modification of membrane properties and fatty acids biosynthesis-related genes in *Escherichia coli* and *Staphylococcus aureus* : Implications for the antibacterial mechanism of naringenin. Biochim. Biophys. Acta-Biomembr. 1860, 481–490.
Wu, H., San, K.Y., 2014. Efficient odd straight medium chain free fatty acid production by metabolically engineered *Escherichia coli*. Biotechnol. Bioeng. 111, 2209–2219.
Xu, C., Wu, P., Gao, J., et al., 2019. Heptadecanoic acid inhibits cell proliferation in PC-9 non small cell lung cancer cells with acquired gefitinib resistance. Oncol. Rep. 41, 3499–3507.
Yu, T., Zhou, Y.J., Huang, M., et al., 2018. Reprogramming yeast metabolism from alcoholic fermentation to lipogenesis. Cell 174, 1549–1558.
Yu, T., Zhou, Y.J., Wenning, L., et al., 2017. Metabolic engineering of *Saccharomyces cerevisiae* for production of very long chain fatty acid-derived chemicals. Nat. Commun. 8, 15587.
Zhang, L.S., Liang, S., Zong, M.H., et al., 2020. Microbial synthesis of functional odd-chain fatty acids: a review. World J. Microb. Biot. 36, 35.
Zhang, Y., Wang, J., Wang, Z., et al., 2019. A gRNA-tRNA array for CRISPR-Cas9 based rapid multiplexed genome editing in *Saccharomyces cerevisiae*. Nat. Commun. 10, 1053.
Zhu, Z.W., Hu, Y.T., Teixeira, P.G., et al., 2020. Multidimensional engineering of *Saccharomyces cerevisiae* for efficient synthesis of medium-chain fatty acids. Nat. Catal. 3, 64–74.